High-Efficiency Low-Bl Loudspeakers

Article · January 2012

CITATIONS
5

READS
1,127

2 authors, including:

R. M. Aarts
Philips
248 PUBLICATIONS **2,333** CITATIONS

SEE PROFILE

High-Efficiency Low-*Bl* Loudspeakers*

RONALD M. AARTS, *AES Fellow*
(ronald.m.aarts@philips.com)

Philips Research Laboratories, 5656AA Eindhoven, The Netherlands

Normally, low-frequency sound reproduction with small transducers is quite inefficient. This is shown by calculating the efficiency and voltage sensitivity for loudspeakers with high, medium, and, in particular, low force factors. For these low-force-factor loudspeakers a practically relevant and analytically tractable optimality criterion, involving the loudspeaker parameters, will be defined. Actual prototype bass drivers are assessed according to this criterion. Because the magnet can be considerably smaller than usual, the loudspeaker can be of the moving-magnet type with a stationary coil. These so-called low-*Bl* drivers have a high efficiency, however, only in a limited frequency region. To deal with that, nonlinear processing essentially compresses the bandwidth of a 20–120-Hz bass signal down to a much more narrow span. This span is centered at the resonance of the low-*Bl* driver, where its efficiency is maximum. The signal processing preserves the temporal envelope modulations of the original bass signal. The compression is at the expense of a decreased sound quality and requires some additional electronics. This new, optimal design has a much higher power efficiency as well as a higher voltage sensitivity than current bass drivers, while the cabinet may be much smaller.

0 INTRODUCTION

The introduction of concepts such as ambient intelligence [1], [2], flat TV, and 5.1-channel sound reproduction systems has led to a renewed interest in obtaining a high sound output from compact loudspeaker arrangements with a high efficiency. Compact relates here to both the volume of the cabinet into which the loudspeaker is mounted and the cone area of the loudspeaker. We will investigate the behavior of transducers for various parameters. It will be shown later that the force factor (*Bl*) of a loudspeaker plays an important role.

To have some qualitative impression, various curves of a medium-*Bl* driver are shown in Fig. 1. We clearly see that there is a band-pass behavior of the acoustical power P_a (fifth curve), and a high-pass response for the on-axis pressure p (third curve), as is typical for medium-*Bl* drivers. In the following we will derive more precise and quantitative relations for the power and pressure response. First we will discuss the efficiency of electrodynamic loudspeakers in general, which will be used later in discussions on special drivers with a high *Bl* value in Section 3 and a very low *Bl* value in Section 4. This low-*Bl* driver can be made very cost-efficient, low-weight, flat, and with high power efficiency. Because *Bl* influences the transient response of normal drivers, and these special low-*Bl* drivers in particular, a transient response analysis is presented in Section 5. But first we show in Section 1 that sound reproduction at low frequencies with small transducers, and at a reasonable efficiency, is very difficult. The reason for this is that the efficiency is inversely proportional to the moving mass and proportional to the square of the product of cone area and force factor *Bl.* All equations presented in this paper are available as MATLAB[1] scripts.[2]

1 EFFICIENCY CALCULATIONS

1.1 Lumped-Element Model

For low frequencies a loudspeaker can be modeled with the aid of some simple elements, allowing the formulation of approximate analytical expressions for the loudspeaker sound radiation. Since we are interested in the power efficiency and voltage sensitivity in particular, we will derive these expressions using this model. The forthcoming loudspeaker model will not be derived here in detail since this has been done elsewhere (see for example, [3]–[11]). The importance of efficiency is discussed widely in the literature in the papers mentioned, but especially in Keele [12], [13] and in particular for efficiency at the resonance

*Manuscript received 2005 April 1; revised 2005 June 15 and June 28.

[1]MATLAB is a trade name of The MathWorks, Inc.
[2]http://www.dse.nl/~rmaarts/.

frequency in Aarts [14]–[16] and in Zuccatti [17], [18]. We first reiterate briefly the theory for the sealed loudspeaker. In what follows, we use a driver model with a simple acoustic air load. The driver is characterized by a cone or piston with radius a and of area

$$S = \pi a^2 \tag{1}$$

and various other parameters, which will be introduced successively and are summarized in Table 1. The radian resonance frequency ω_0 is given by

$$\omega_0 = \sqrt{\frac{k_t}{m_t}} \tag{2}$$

where m_t is the total moving mass including the air load and k_t is the total spring constant of the system, including the loudspeaker and possibly its enclosing cabinet of volume V_0. This cabinet exerts a restoring force on the piston with the equivalent spring constant

$$k_B = \frac{\gamma P_0 S^2}{V_0} = \frac{\rho c^2 S^2}{V_0} \tag{3}$$

where γ is the ratio of the specific heats (1.4 for air), P_0 the atmospheric pressure, ρ the density, and c the speed of sound of the medium.

The relation between the driving voltage $e(t)$, the current $i_c(t)$, and the piston displacement $x(t)$ is given by

$$e(t) = R_e i_c(t) + Bl\frac{dx(t)}{dt} + L_e\frac{di_c(t)}{dt} \tag{4}$$

where R_e is the voice-coil resistance, Bl the force factor, and L_e the self-inductance of the voice coil. This force factors is equal to the product of the flux density B in the air gap and the effective length l of the voice-coil wire. We will see later that $(Bl)^2/R_e$ appears in many formulas; it has the dimension of mechanical ohms [kg/s]. The term Bl is called force factor because the electromagnetic Lorentz force F acting on the voice coil is given by $F = Bli_c$. The term including dx/dt is the voltage induced by the driver piston velocity of motion. Using the Laplace transform, Eq. (4) can be written as

$$E(s) = R_e I_c(s) + BlsX(s) + L_e s I_c(s) \tag{5}$$

where capital letters are used for the corresponding Laplace transformed variables, and s is the Laplace variable, which can be replaced by $i\omega$ for stationary harmonic signals. The relation between the mechanical forces and the electrical driving force is given by

$$m_t\frac{d^2x}{dt^2} + R_m\frac{dx}{dt} + k_t x = Bli_c \tag{6}$$

Table 1. System parameters of model presented in Fig. 2.

B	Flux density in air gap
Bl	Force factor
E	Voice-coil voltage
F	Lorentz force acting on voice coil
i	$=\sqrt{-1}$
I_c	Voice-coil current
k_t	Total spring constant, $=k_d$ (driver alone) + k_B (box)
l	Effective length of voice-coil wire
L_e	Self-inductance of voice coil
m_t	Total moving mass, including air-load mass
R_e	Electrical resistance of voice coil
R_m	Mechanical damping
R_d	Electrodynamic damping, $=(Bl)^2/R_e$
R_t	Total damping, $= R_r + R_m + R_d$
U	Voltage induced in voice coil
V	Velocity of the voice coil
Z_{rad}	Mechanical radiation impedance, $=R_r + iX_r$

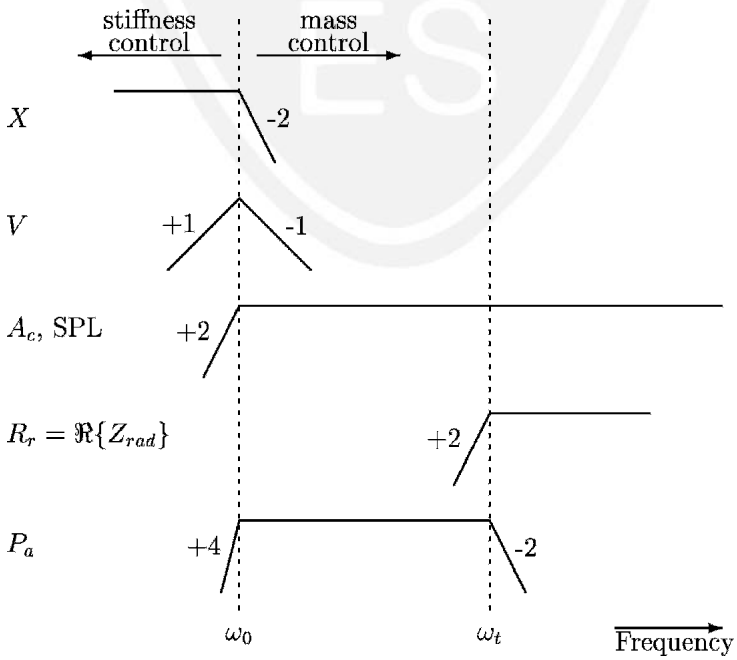

Fig. 1. Displacement X, velocity V, acceleration $A_c = sV$ together with on-axis SPL, real part of radiation impedance $R_r = \Re\{Z_{rad}\}$, and acoustical power P_a of a rigid-plane piston in an infinite baffle, driven by a constant force (from [3]). Numbers denote slopes of curves. Multiplied by 6 these yield slope in dB/octave. ω_t is transition frequency defined by Eq. (20).

where on the left-hand side we have the mechanical forces, which are the inertial reaction of the cone with total moving mass m_t, the mechanical resistance R_m, and the total spring force with total spring constant k_t; on the right-hand side we have the external electromagnetic Lorentz force $F = Bli_c$. For the moment we assume that the radiation resistance R_r (which is very small) is included in R_m; where appropriate we will mention it explicitly. Combining Eq. (5) and the Laplace transform of Eq. (6) we get

$$X(s)\left\{s^2 m_t + s\left[R_m + \frac{(Bl)^2}{L_e s + R_e}\right] + k_t\right\} = \frac{BlE(s)}{L_e s + R_e}. \quad (7)$$

We see that besides the mechanical damping R_m we also get an electrodynamic damping term $(Bl)^2/(L_e s + R_e)$, and this term plays an important role. If we ignore the self-inductance of the loudspeaker and the effect of eddy currents, we can write Eq. (7) as the transfer function $H_x(s)$ between voltage $E(s)$ and displacement $X(s)$,

$$H_x(s) = \frac{X(s)}{E(s)} = \frac{Bl/R_e}{s^2 m_t + s[R_m + (Bl)^2/R_e] + k_t}. \quad (8)$$

We assume an infinite baffle to mount the piston, and in the compact-source regime ($a/r << \lambda/a$, where λ is the wavelength) the far-field acoustic pressure $p(t)$ at a distance r becomes

$$p(t) = \frac{\rho S(d^2x/dt^2)}{2\pi r} \quad (9)$$

showing that $p(t)$ is proportional to the volume acceleration of the source [19], [20]. In the Laplace domain we have

$$P(s) = \frac{s^2\, \rho S X(s)}{2\pi r}. \quad (10)$$

Using Eq. (10) and neglecting the self-inductance L_e we can write Eq. (7) as the transfer function from voltage to pressure,

$$H_p(s) = \frac{P(s)}{E(s)} = \frac{s^2\, \rho S/(2\pi r) Bl/R_e}{s^2 m_t + s[R_m + (Bl)^2/R_e] + k_t}. \quad (11)$$

With the aid of Eqs. (5) and (8) and the properties of the gyrator, as shown in Fig. 2, the electrical impedance $Z_{in}(\omega)$ of the loudspeaker can be calculated,

$$Z_{in}(\omega) = R_e + i\omega L_e + \frac{(Bl)^2}{(R_m + R_r) + i\omega m_t + k_t/(i\omega)}. \quad (12)$$

Using the following relations of dimensionless quality factors Q, dimensionless frequency detuning ν, and time constant τ_e,

$$Q_m = \frac{\sqrt{k_t m_t}}{R_m}, \quad Q_e = \frac{R_e\sqrt{k_t m_t}}{(Bl)^2}, \quad Q_r = \frac{\sqrt{k_t m_t}}{R_r}$$
$$Q_{mr} = \frac{Q_m Q_r}{Q_m + Q_r}, \quad \nu = \frac{\omega}{\omega_0} - \frac{\omega_0}{\omega}, \quad \tau_e = \frac{L_e}{R_e} \quad (13)$$

we can write Z_{in} as

$$Z_{in}(\omega) = R_e\left(1 + i\omega\tau_e + \frac{Q_{mr}/Q_e}{1 + iQ_{mr}\nu}\right). \quad (14)$$

If we neglect L_e, we get at the resonance frequency ($\omega = \omega_0$ or $\nu = 0$) the maximum input impedance

$$Z_{in}(\omega_0) = R_e\left(1 + \frac{Q_{mr}}{Q_e}\right) \approx R_e + \frac{(Bl)^2}{R_m}. \quad (15)$$

From this we see that Bl plays an important role in the electrical impedance, which is most pronounced at the resonance frequency.

1.2 Efficiency and Voltage Sensitivity

In order to calculate the power efficiency of a loudspeaker we need to calculate the electric power delivered to the driver as well as the acoustical power delivered by the loudspeaker. The latter depends on the radiation impedance of the driver. We now calculate these three functions.

The time-averaged electric power P_e delivered to the driver can be written as

$$P_e = 0.5\,|I_c|^2 \Re\{Z_{in}\} = 0.5\,|I_c|^2 R_e\left(1 + \frac{Q_{mr}/Q_e}{1 + Q_{mr}^2\nu^2}\right) \quad (16)$$

where $\Re\{Z_{in}\}$ is the real (resistive) part of the input impedance Z_{in}. The radiation impedance Z_{rad} of a plane circular rigid piston with radius a in an infinite baffle can be derived as [19, p. 384]

$$Z_{rad} = \pi a^2 \rho c\left[1 - \frac{2J_1(2ka)}{2ka} + \frac{i2\mathbf{H}_1(2ka)}{2ka}\right] \quad (17)$$

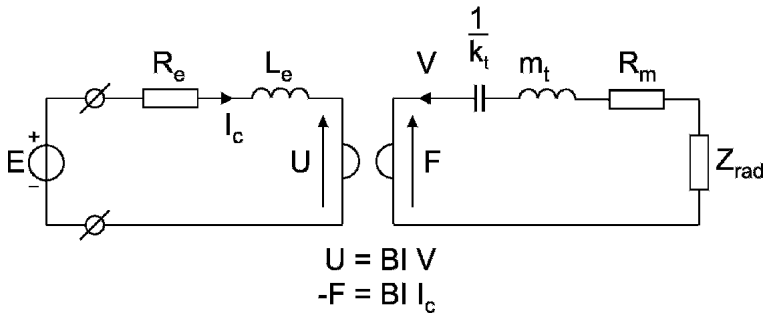

Fig. 2. Lumped-element model of impedance-type analogy of an electrodynamic loudspeaker. Coupling between electrical and mechanical parts is represented by a gyrator. For system parameters see Table 1.

where $\mathbf{H}_1$ is a Struve function, J_1 is a Bessel function [21, §12.1.7 and §9], and k is the wavenumber ω/c. An accurate full-range approximation of $\mathbf{H}_1$ is given in [22] as

$$\mathbf{H}_1(z) \approx \frac{2}{\pi} - J_0(z) + \left(\frac{16}{\pi} - 5\right)\frac{\sin z}{z} + \left(12 - \frac{36}{\pi}\right)\frac{1-\cos z}{z^2}. \tag{18}$$

The real and imaginary parts of Z_{rad} are plotted in Fig. 3. Z_{rad} can be approximated as [5], [22]

$$Z_{\text{rad}} \approx \begin{cases} \pi a^2 \rho c\left[\dfrac{(ka)^2}{2} + \dfrac{\mathrm{i}8ka}{3\pi}\right], & \omega << \omega_t \\ \pi a^2 \rho c\left(1 + \dfrac{\mathrm{i}2}{\pi ka}\right), & \omega >> \omega_t \end{cases} \tag{19}$$

where

$$\omega_t = \frac{1.4c}{a} \tag{20}$$

is the transition frequency (−3-dB point). For low frequencies ($\omega \ll \omega_t$) we can either neglect the damping influence of Z_{rad} or (assuming $c = 343$ m/s and $\rho = 1.21$ kg/m^3) use as a rule of thumb

$$R_r = \Re\{Z_{\text{rad}}\} \approx (0.15Sf)^2. \tag{21}$$

This follows immediately from Eq. (19) and has an error of less than 2%. We see that R_r is indeed rising with frequency with slope 2, as qualitatively depicted in Fig. 1, and is proportional to the fourth power of the radius a. The real part of Z_{rad} is plotted more accurately in Fig. 3.

The time-averaged acoustically radiated power can then be calculated as

$$P_a = 0.5|V|^2\Re\{Z_{\text{rad}}\} \tag{22}$$

which, using Eqs. (8), (13), and $V = sX$, can be written as

$$P_a = \frac{0.5[Bl/(R_m + R_r)]^2 I_c{}^2 R_r}{1 + Q_{mr}^2 \nu^2}. \tag{23}$$

The qualitative behavior of this function is depicted in Fig. 1.

To investigate the exact behavior of the sound pressure, rather than its qualitative behavior (third curve in Fig. 1), we will derive the necessary equations for the pressure—first in general, then for low frequencies. The acoustic pressure due to the piston in the far field at distance r and azimuth angle θ, assuming an axis of symmetry at $\theta = 0$ rad, is

$$p(r,t) = \mathrm{i}\frac{\omega\rho V\pi a^2}{2\pi r}\left[\frac{J_1(ka\sin\theta)}{ka\sin\theta}\right]\mathrm{e}^{\mathrm{i}\omega(t-r/c)} \tag{24}$$

where V is the velocity of the piston [5], [20]. The velocity profile V is depicted in Fig. 1, which we use to calculate the magnitude of the on-axis response ($\theta = 0$). This is also depicted in Fig. 1, which shows a "flat" SPL for $\omega \gg \omega_0$. However, due to the term in square brackets in Eq. (24), the off-axis pressure response ($\theta \neq 0$) decreases with increasing ka. This yields an upper frequency limit for the acoustical power, together with the mechanical lower frequency limit ω_0, which is the reason why a practical loudspeaker system needs more than one driver (a multiway system) to handle the whole audible frequency range.

Assuming that there is no directivity ($|ka\sin\theta| \ll 1$), leaving out the phase term in Eq. (24), and using the relations between velocity, current, and voltage as before, we get the pressure (voltage) sensitivity $H_p(\omega)$,

$$H_p(\omega) = \frac{P(\omega)}{E(\omega)} = \frac{(\mathrm{i}\omega)^2}{(\mathrm{i}\omega)^2 m_t + \mathrm{i}\omega R_t + k_t}\frac{\rho a^2 Bl}{2r R_e} \tag{25}$$

or

$$H_p(\omega) = \frac{(\mathrm{i}\omega/\omega_0)^2}{(\mathrm{i}\omega/\omega_0)^2 + (\mathrm{i}\omega/\omega_0)Q_t^{-1} + 1}\left(\frac{\rho a^2 Bl}{2m_t r R_e}\right) \tag{26}$$

with the total quality factor $Q_t = m_t\omega_0/R_t$. Eq. (26) clearly shows the frequency-dependent high-pass behavior in its first factor and a frequency-independent sensitivity in the second factor. The latter shows that in order to have a high sensitivity, a^2Bl must be high and $2m_tR_e$ must be low, which means a big and expensive loudspeaker (because of the magnet). A much more attractive situation occurs at resonance ($\omega = \omega_0$). Then Eq. (26) becomes

$$\frac{P(\omega_0)}{E(\omega_0)} = \frac{\mathrm{i}\rho a^2 BlQ_t}{2m_t r R_e}. \tag{27}$$

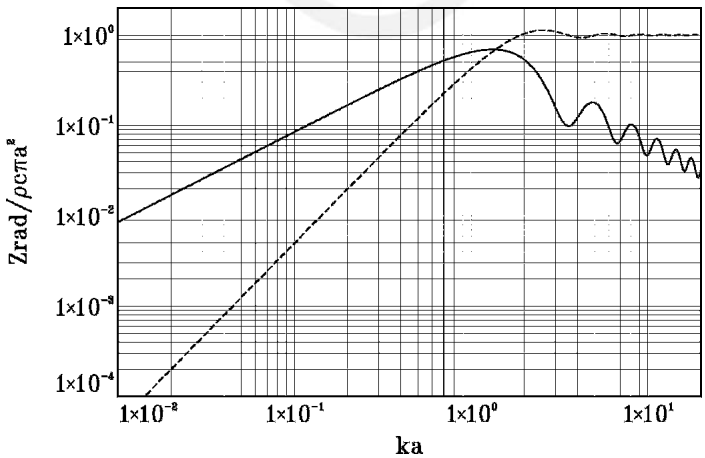

Fig. 3. Real (- - -) and imaginary (——) parts of normalized radiation impedance of rigid disk having radius a in an infinite baffle, using Eqs. (17), (18), and $k = \omega/c$.

In Section 4.1 we will elaborate on this, and we will show that at the resonance frequency it is beneficial to have a low *Bl* value.

Using Eqs. (16) and (23) the power efficiency can now be calculated as

$$\eta(\nu) = \frac{P_a}{P_e} = \left[Q_e Q_r \left(\nu^2 \frac{+1}{Q_{mr}^2} \right) + \frac{Q_r}{Q_{mr}} \right]^{-1}. \quad (28)$$

In the following section the influence on efficiency is discussed for various *Bl* values while the other parameters remain the same.

A convenient way to relate the sound pressure level (SPL) to the power activity η is the following. For a plane wave we have the relation between sound intensity I and sound pressure p,

$$I = \frac{p^2}{\rho c} \quad (29)$$

and the acoustical power is equal to

$$P_a = 2\pi r^2 I = \frac{2\pi r^2 p^2}{\rho c}. \quad (30)$$

Using these relations we get for the SPL

$$\mathrm{SPL} = 20 \log \left(\sqrt{\frac{P_a \rho c}{2\pi r^2}} \Big/ p_0 \right) \quad (31)$$

where we assume radiation into one hemifield (solid angle of 2π), that is, we only account for the pressure at one side of the cone, which is mounted in an infinite baffle. For $r = 1$ m, $\rho c = 415$ kg/(m$^2 \cdot$ s), $P_a = 1$ W, and $p_0 = 20 \times 10^{-6}$ Pa, we get

$$\mathrm{SPL} = 112.18 + 10 \log \eta. \quad (32)$$

If $\eta = 1$ (in this case $P_a = P_e = 1$ W), we get the maximum attainable SPL of 112.18 dB. Eq. (32) can also be used to calculate η if the SPL for $P_e = 1$ W is known, such as by measurement.

2 SPECIAL DRIVERS FOR LOW FREQUENCIES

In this section two options are described whereby modifying a conventional loudspeaker driver can lead to enhanced bass perception. This is achieved by modifying the force factor of the driver, typically by using either a very strong or a very weak magnet compared to what is commonly used in typical drivers. Both these approaches also require some preprocessing of the signal before it is applied to the modified loudspeaker. In Section 2.1 the influence of the force factor on the performance of the loudspeaker is reviewed. Then Sections 3 and 4 discuss high-force-factor and low-force-factor drivers, respectively, and their required signal processing. Section 5 presents an analysis of the transient responses of normal drivers and these special ones.

2.1 Force Factor

Direct-radiator loudspeakers typically have a very low efficiency because the acoustic load on the diaphragm or cone is relatively low compared to the mechanical load. In addition, the driving mechanism of a voice coil is quite inefficient in converting electric energy into mechanical motion. The force factor *Bl* is deliberately kept at an intermediate level so that the typical response is flat enough—like the third curve in Fig. 1—to use the device without significant equalization. It was already shown in Section 1 that the force factor *Bl* plays an important role in loudspeaker design. It determines among other features the frequency response and its related transient response, the electrical input impedance, the cost, and the weight of the loudspeaker. We will discuss several of these consequences.

To show the influence on the frequency response, the SPL of a driver with three *Bl* values (low, medium, and high) is plotted in Fig. 4. All other parameters are being kept constant and are listed in Table 2.[3] It appears that the curves change drastically for varying *Bl.* The most prominent difference is the shape, but also the difference in level at high frequencies is apparent. While the low-*Bl* driver has the highest response at the resonance frequency, it has a poor response beyond resonance, which requires special treatment, as will be discussed in Section 4.1. The high-*Bl* driver has a good response at higher frequencies, but a poor response at lower frequencies. which requires special equalization, as will be discussed in Section 3.1. In between we have the well-known curve for a medium-*Bl* driver.

To show the influence of *Bl* on the electrical input impedance, its magnitude is plotted in Fig. 5 for a driver with three *Bl* values (low, medium, and high), all other parameters being kept the same. It appears that these curves also change drastically for varying *Bl.* This is also true for the phase of the electrical input impedance, which is plotted in Fig. 6.

The underlying reason for the importance of *Bl* is that besides determining the driving force, it also gives (electrodynamic) damping to the system. The total damping is equal to the sum of the (real part of the) radiation impedance, the mechanical damping, and the electrodynamic damping $(Bl)^2/R_e$, where the electrodynamic damping dominates for medium- and high-*Bl* loudspeakers, and is most prominent around the resonance frequency. The power efficiency given in Eq. (28) can be written as

$$\eta = \frac{(Bl)^2 R_r}{R_e\{(R_m + R_r)^2 + (R_m + R_r)(Bl)^2/R_e + (m_t \omega_0 \nu)^2\}}. \quad (33)$$

[3]Table 2 lists the lumped parameters for various low-frequency loudspeakers (woofers) with diameters of 4, 7, 8, and 12 in (0.1, 0.18, 0.2, and 0.3 m), some having a low or a high Q_e. Two special drivers are also listed—an (optimal) low-*Bl* (MM3c) and a high-*Bl* driver (HB1). The former is an experimental driver (see Fig. 8 for its compact magnet system). The efficiency of the drivers listed in the table is in the range of 0.2–10%. As a rule of thumb, we see that for these drivers $k_d \approx 1$ N/mm, m_t [g] $= c_m S$ ($c_m \approx 0.1$ g/cm^2), and $R_m \approx 1$ Ns/m, while the other parameters may differ significantly between the various drivers. See Table 1 for the abbreviations and the meaning of the variables.

If $(m_t\omega_0\nu)^2 >> (R_m + R_r)^2 + (R_m + R_r)(Bl)^2/R_e$, and R_r is approximated by Eq. (19), then Eq. (33) can be written as

$$\eta(\omega_0 << \omega << \omega_t) \approx \frac{(Bl)^2 S^2 \rho}{2\pi c R_e m_t^2}. \quad (34)$$

This is a well-known result in the literature and clearly shows the influence of *Bl.* However, it is valid in a limited frequency range only. Using Eq. (33) the power efficiency η is plotted in Fig. 7, which clearly shows the dependence on frequency. Three *Bl* values (low, medium, and high) are used, while all other parameters are being kept the same. It appears that the curves change drastically for varying *Bl,* but only very modestly around the resonance frequency. This can be elucidated further by using Eq. (33) at the resonance frequency and assuming that $R_m + R_r \ll (Bl)^2/R_e$. We then get

$$\eta(\omega = \omega_0) \approx \frac{R_r}{R_m + R_r}. \quad (35)$$

Eq. (35) shows the value of the power efficiency at the resonance frequency for sufficiently large values of *Bl,* and indeed the three curves of Fig. 7 are almost coincident, even for the low-*Bl* curve.

The importance of *Bl* is further elucidated in the following section as well as in Section 5, where the transient response is calculated. The latter appears to be dependent on *Bl* as well.

3 HIGH-FORCE-FACTOR DRIVERS

A part of this section is excerpted directly from [23], which includes a more detailed analysis of high-*Bl* drivers. In the 1990s a new rare-earth-based material, neodymium–iron–boron (NdFeB), in sintered form, came into more common use. It has a very high flux density coupled with a high coercive force, possessing a *BH* product increased by almost an order of magnitude compared to more common materials. This allows drivers to be built in practice with much larger total magnetic flux, thereby increasing *Bl* by a large factor. In [23] some features of normal sealed-box loudspeakers with greatly increased *Bl* were outlined. While that paper focused mainly on the efficiency of the system as applied to several amplifier types, several other

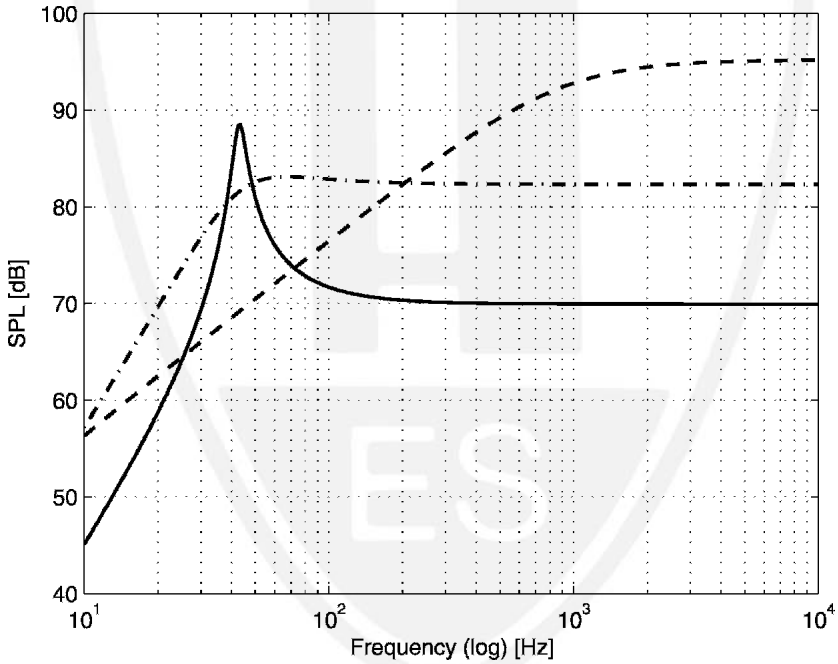

Fig. 4. Sound pressure level (SPL) for driver MM3c with three *Bl* values: low *Bl* = 1.2 (——), medium *Bl* = 5 (- · - · -), and high *Bl* = 22 N/A (- - -). All other parameters are kept as given in Table 2; all with 1 W input power. At resonance frequency, the highest SPL is obtained by the low-*Bl* driver, the high-*Bl* driver having a poor response.

Table 2. Lumped parameters for various low-frequency loudspeakers.[3]

Type	R_e (Ω)	Bl (T · m)	k_d (N/m)	m_t (g)	R_m (N · s/m)	S (cm^2)	f_0 (Hz)	Q_m	Q_e
AD44510	6.6	3.5	839	4	0.86	54	72	2.2	1.02
AD70801	6.9	2.9	1075	6.3	0.81	123	66	3.2	2.13
AD80110	6.0	9.0	971	16.5	1.38	200	39	2.9	0.29
AD80605	6.8	5.1	1205	13.4	0.84	200	48	4.8	1.05
AD12250	6.6	13.0	1429	54.0	2.93	490	26	3.0	0.34
AD12600	6.9	6.0	1205	33.0	0.76	490	31	8.2	1.21
MM3c	6.4	1.2	1022	14.0	0.22	86	43	17.2	16.8
HBl	7.5	22.0	3716	56.0	0.91	490	41	16.0	0.22

avenues of interest were also indicated. Fig. 4 shows the frequency response curves [using Eqs. (10) and (11)] for the three *Bl* values of 1.2. 5.0, and 22 N/A. At the higher *Bl* value the electromagnetic damping is very high. If we ignore in this case the small mechanical and acoustic damping of the driver, the damping term is proportional to $(Bl)^2/R_e$. For a Butterworth response the inertial term $\omega^2 m_t$, the damping term $\omega(Bl)^2/R_e$, and the total spring constant k_t are all about the same at the bass cutoff frequency. When *Bl* is increased by a factor of 5, the damping is increased by a factor of 25. Thus the inertial factor, which dominates at high frequencies. becomes equal to the damping at a frequency about 25 times higher than the original cutoff frequency. This causes the flat response of the system to have a 6-dB per octave rolloff below that frequency, as shown in Fig. 4.

At very low frequencies the spring restoring force becomes important relative to the damping force at a frequency 25 times lower than the original cutoff frequency. Below this the rolloff is 12 dB per octave. Such frequencies are too low to influence audio performance, but it is clear that the system stiffness (driver and cabinet) is

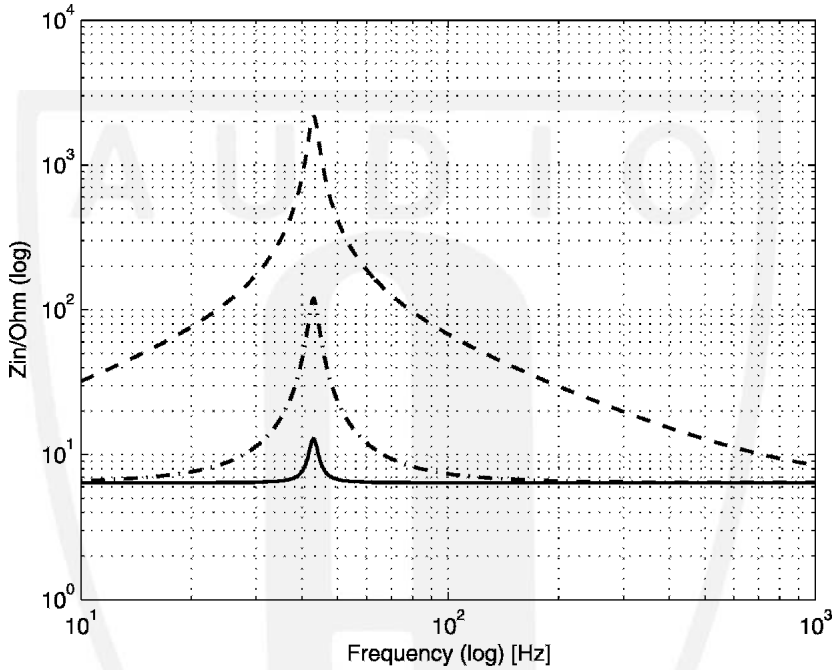

Fig. 5. Magnitude of electrical input impedance for driver MM3c with three *Bl* values: low *Bl* = 1.2 (——), medium *Bl* = 5 (- · - · -), and high *Bl* = 22 N/A (---). All other parameters are kept as given in Table 2.

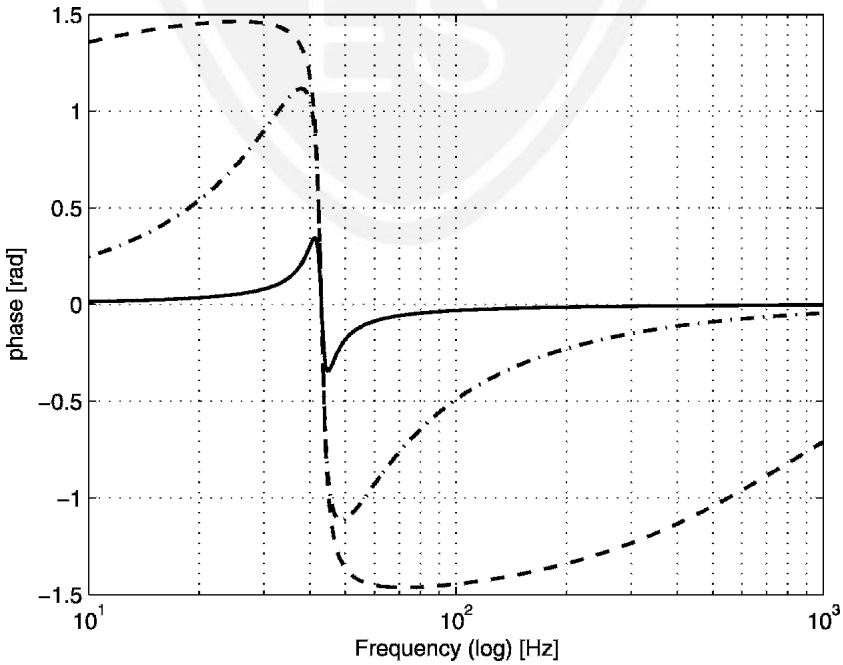

Fig. 6. Phase of electrical input impedance for driver MM3c with three *Bl* values: low *Bl* = 1.2 (——), medium *Bl* = 5 (- · - · -), and high *Bl* = 22 N/A (---). All other parameters are kept as given in Table 2.

now no longer constraining the low-frequency performance. We could use a much smaller box without serious consequences.

How much smaller can the box be? The low-frequency cutoff has been moved down by a factor of nearly 25. The driver suspension stiffness k_d is small, and because the cabinet suspension stiffness k_B is proportional to $1/V_0$, the cutoff frequency will return to the initial bass cutoff frequency when the box size is reduced by a factor of about 25: a 25-l box could be reduced to 1 l. Powerful electrodynamic damping has allowed the box to be reduced in volume without sacrificing the response at audio frequencies. The only penalty is that we must apply some equalization.

The equalization needed to restore the response to the original value can be deduced from Fig. 4, because the required equalization is the difference between the $Bl = 5$ (dash–dot) and $Bl = 22$ N/A (dashed) curves. Such equalization will, in virtually all cases, increase the voltage applied to the loudspeaker, because the audio energy resides principally at lower frequencies.

The power efficiency for very large Bl can be calculated [using Eq. (33)] as

$$\lim_{Bl\to\infty} \eta = \frac{R_r}{R_m + R_r}. \tag{36}$$

This clearly shows that the efficiency increases for decreased mechanical damping R_m.

3.1 An Observation about Equalization

The required equalization can be calculated by the frequency response ratio $H_{p,L}(\omega)/H_{p,H}(\omega)$ using Eq. (11), where the subscripts H and L refer to the high and low values of Bl. The required equalization function for two loudspeakers with different Bl values, but identical in all other respects, can also be calculated using a different approach. There holds

$$H_{EQ}(\omega) = \frac{(Bl)_L/Z_{in,L}(\omega)}{(Bl)_H/Z_{in,H}(\omega)} \tag{37}$$

where the subscripts H and L at the electrical input impedance Z_{in} refer to the high and low values of Bl used. Note that it applies to the response at any orientation, not just on axis, and represents a general property of acoustic transducers with magnetic drivers, including that of low-Bl drivers to be discussed in the next section.

4 LOW-FORCE-FACTOR DRIVERS

As explained before, normally low-frequency sound reproduction with small transducers is quite inefficient. To increase the efficiency two measures are taken. First, nonlinear processing essentially compresses the bandwidth of a 20–120-Hz bass signal down to a much narrower span. This span is centered at the resonance of the low-Bl driver, where its efficiency is maximum. Second, a special transducer is used with a low Bl value, attaining a very high efficiency at that particular frequency. Therefore these drivers are only useful for subwoofers. In the following an optimum force factor is derived to obtain such a result.

4.1 Optimum Force Factor

Our proposed solution to obtain a high sound output from a compact loudspeaker arrangement, with a good efficiency, consists of two steps. First, the requirement that the frequency response be flat is relaxed. By making the magnet considerably smaller and lighter (see Fig. 8 at right) a large peak in the SPL curve (solid curve in Fig. 4)

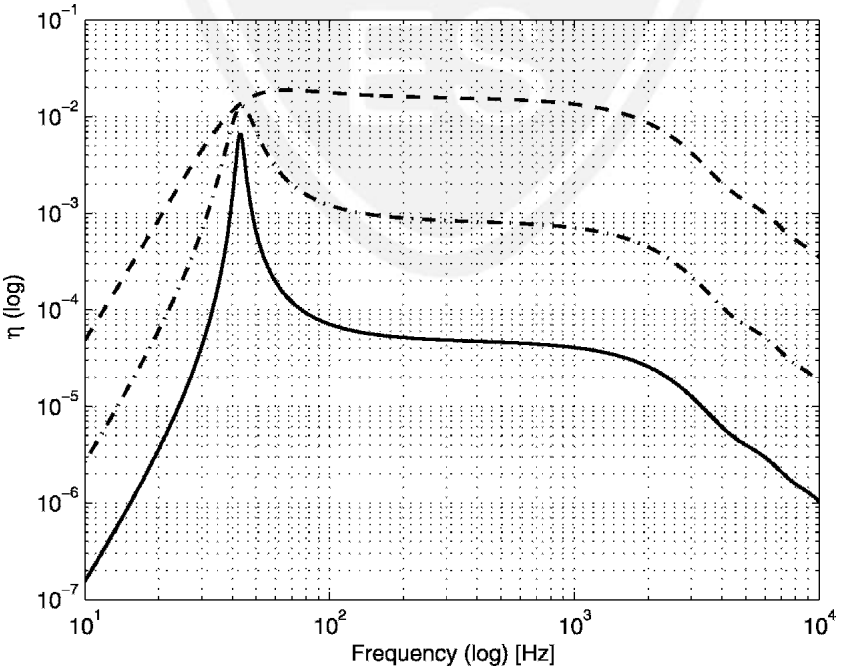

Fig. 7. Power efficiency η for driver MM3c with three Bl values: low $Bl = 1.2$ (——), medium $Bl = 5$ (- · - · -), and high $Bl = 22$ N/A (- - -). All other parameters are kept as given in Table 2. Note that efficiency is strongly dependent on Bl at all frequencies except at resonance, where it is affected only modestly by Bl.

will appear. Because the magnet can be considerably smaller than usual, the loudspeaker can be of the moving-magnet type with a stationary coil (see Fig. 8) instead of vice versa. At the resonance frequency the voltage sensitivity can be a factor of 10 higher than that of a normal loudspeaker. In this case we have, at the resonance frequency of about 40 Hz, an SPL of almost 90 dB at 1 W input power and 1 m distance, even when using a small cabinet. An example is shown in Fig. 9. Because it is operating in resonance mode only, the moving mass can be enlarged (which might be necessary owing to the small cabinet) without degrading the efficiency of the system.

Due to the large and narrow peak in the frequency response, the normal operating range of the driver decreases considerably. This makes the driver unsuitable for normal use. To overcome this, a second measure is applied. The nonlinear processing essentially compresses the bandwidth of a 20–120-Hz 2.5-octave bass signal down to a much narrower span. This span is centered at the resonance of the low-*Bl* driver, where its efficiency is maximum [15], [16]. This can be done with a setup such as depicted in Fig. 10.

The modulation is chosen such that the coarse structure (the envelope) of the music signal after compression, or "mapping," is the same as before the mapping. An example is shown in Fig. 11. Fig. 11(a) shows the waveform of a rock-music excerpt; the thin curve depicts its envelope. Fig. 11(b) and (c) presents the spectrograms of the input and output signals, respectively, clearly showing that the frequency bandwidth of the signal around 60 Hz decreases after the mapping, yet the temporal modulations remain the same.

Using Eqs. (8) and (10), the voltage sensitivity at the resonance frequency can be written as

$$H_{\mathrm{p}}(\omega_0) = \frac{P(\omega_0)}{E(\omega_0)} = \frac{\mathrm{i}\omega_0 SBl\rho}{2\pi r R_{\mathrm{e}}[R_{\mathrm{m}} + (Bl)^2/R_{\mathrm{e}}]}. \tag{38}$$

If Eq. (38) is maximized by adjusting the force factor *Bl* by differentiating $H(\omega = \omega_0)$ with respect to *Bl* and setting

Fig. 8. Prototype driver (MM3c) with a 10 Euro cent coin. At the position where a normal loudspeaker has its heavy and expensive magnet, the prototype driver has an almost empty cavity. Only a small moving magnet is necessary, which is shown at right.

Fig. 9. Prototype bass transducer (MM800) in 1-1 cabinet (1-Euro coin for size comparison, lower left-hand corner) with a resonance frequency of 55 Hz.

$\partial H/\partial(Bl) = 0$, we get

$$\frac{(Bl)^2}{R_e} = R_m. \tag{39}$$

Note at this point that if Eq. (39) holds, we get for this particular case $Q_e = Q_m$ [see Eq. (13)]. It appears that the maximum voltage sensitivity is reached as the electrodynamic damping term $(Bl)^2/R_e$ is equal to the mechanical damping term R_m. In this case we refer to the optimum force factor as

$$(Bl)_o = \sqrt{R_e R_m}. \tag{40}$$

If Eq. (39) is substituted into Eq. (38), this yields the optimal voltage sensitivity ratio

$$H_o(\omega = \omega_0) = \frac{i\omega_0 \rho S}{4\pi r (Bl)_o}. \tag{41}$$

We find that the specific relationship between $(Bl)_o$ and both R_m and R_e [Eq. (39)] causes H_o to be inversely proportional to $(Bl)_o$ (which may seem counterintuitive), and thus also inversely proportional to $\sqrt{R_m}$.

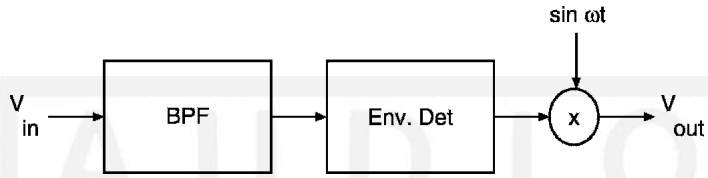

Fig. 10. Frequency mapping scheme. BPF—band-pass filter; Env. Det—envelope detector; signal V_{out} is fed to driver (via a power amplifier).

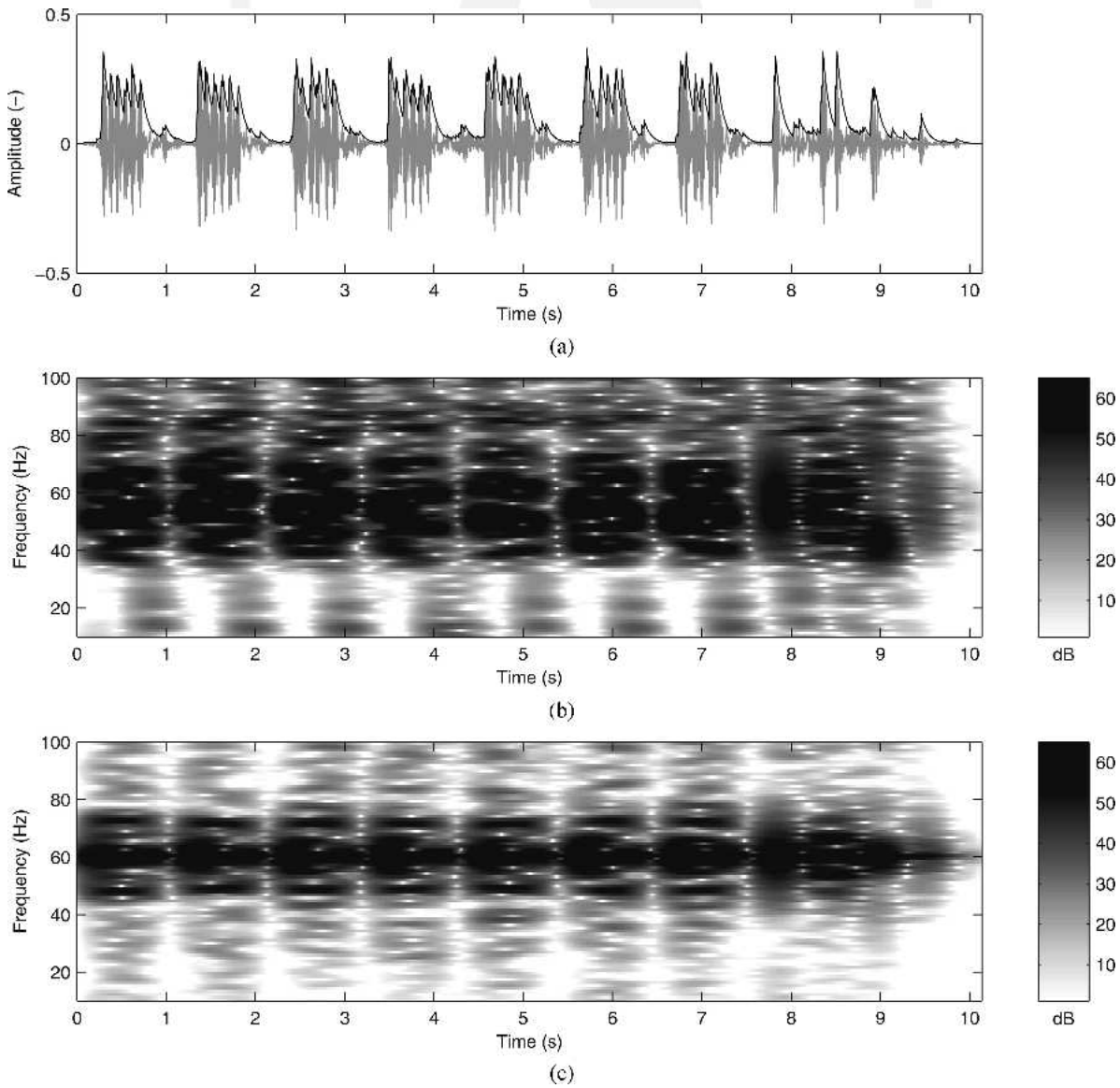

Fig. 11. Signals before and after frequency-mapping processing of Fig. 10. (a) Time signal at V_{in}; thin curve—output of envelope detector. (b) Spectrogram of input signal. (c) Spectrogram of output signals.

The power efficiency at the resonance frequency under the optimality condition obtained by substitution of Eq. (39) into Eq. (33) yields

$$\eta_o(\omega = \omega_0) = \frac{R_m R_r}{(R_m + R_r)^2 + (R_m + R_r)R_m}. \quad (42)$$

This can be approximated for $R_r << R_m$ as

$$\eta_o(\omega = \omega_0) \approx \frac{R_r}{2R_m} \quad (43)$$

which clearly shows that for a high power efficiency at the resonance frequency the cone area must be large, because R_r is—according Eq. (17)—proportional to the squared cone area; and that the mechanical damping must be as small as possible. The damping must be not too small, because the transient response depends on the damping as well, as will be discussed in the next section. This conclusion is the same as for achieving optimum voltage sensitivity [given by Eq. (41)].

Using Eqs. (10), (11), (39), and $V = sX$, we get for the cone velocity sensitivity

$$\frac{V_o(\omega_0)}{E(\omega_0)} = \frac{1}{2(Bl)_o} \quad (44)$$

which again shows the benefit of low Bl and R_m values. Furthermore, assuming the optimality condition given by Eq. (39) and using Eq. (15), we get

$$Z_{o,in}(\omega_0) \approx 2R_e \quad (45)$$

which clearly shows that the peak in the impedance curve is equal to twice that of R_e.

Using Eq. (39) we get a high efficiency. This is at the expense of a decreased sound quality and some additional electronics to accomplish the frequency mapping. However, listening tests confirmed that the decrease in sound quality appears to be modest, as will be discussed in Section 6.

5 TRANSIENT RESPONSE

Because Bl influences the transient response of normal drivers and low-Bl drivers in particular, a transient response analysis is presented next. In [24] the response to a sinusoid which is switched on at $t = 0$ was calculated. Those results showed that the medium- and high-Bl driver systems rapidly converge to their steady-state response, while this is not generally the case for low-Bl drivers. This can also be seen by calculating the impulse response. The transfer function $H_x(s)$, from voltage E to displacement X [Eq. (8)], can be written as

$$H_x(s) = \frac{Bl/R_e}{s^2 m_t + sR_t + k_t} \quad (46)$$

where m_t is the total moving mass, R_t is the total damping (mechanical, electrodynamic, and acoustical),

$$R_t = R_m + \frac{(Bl)^2}{R_e} + R_r \quad (47)$$

and k_t is the total spring constant, as described in Section 1. Knowing that the Laplace transform for a sinusoid with amplitude A and frequency ω_s is

$$E(s) = \frac{A\omega_s}{s^2 + \omega_s^2} \quad (48)$$

$X(s)$ can be calculated as

$$X(s) = \frac{(Bl/R_e)\, A\omega_s/(s^2 + \omega_s^2)}{s^2 m_t + sR_t + k_t}. \quad (49)$$

Assuming that $R_t^2 < 4\, m_t k_t$, the right-hand side of Eq. (46) has complex conjugate poles $s_{1,2}$, given by

$$s_{1,2} = -\beta\omega_0 \pm i\omega_n = -a \pm ib \quad (50)$$

where β is the damping,

$$b^2 = \omega_n^2 = \frac{k_t}{m_t} - \left(\frac{R_t}{2m_t}\right)^2 \quad (51)$$

is the natural frequency, and

$$a = \frac{R_t}{2m_t}. \quad (52)$$

Here we see that the time constant a^{-1} is proportional to the total moving mass m_t—therefore tweeter domes must be light and woofers need not be very light—and inversely proportional to the total damping. The response (displacement versus time) to a sinusoid that is switched on at $t = 0$ is plotted in Fig. 12 (solid curve). The figure shows that it takes some time—which is proportional to the time constant a^{-1}—before the displacement is settled to its final value.

5.1 Impulse Response

The impulse response $h(t)$ of the cone displacement can be calculated directly by the inverse Laplace transform of $H_x(s)$ [Eq. (46)]. There are three possibilities for the poles of Eq. (46): they can be complex, real and equal, or real and separate. We will consider all three.

5.1.1 Complex Poles

If $R_t^2 < 4m_t k_t$, then the poles of Eq. (46) are complex and given by Eq. (50) as discussed. The corresponding impulse response is equal to

$$h(t) = \frac{K_1}{\omega_n} e^{-at} \sin(\omega_n t) \quad (53)$$

where $K_1 = Bl/(R_e m_t)$. Fig. 13 shows the impulse response curves, using Eq. (53) for low (solid curve) and medium (dash–dot curve) Bl drivers with Bl values of 1.2 and 5.0 N/A.

5.1.2 Real and Equal Poles

If $R_t^2 = 4m_t k_t$, then the poles of Eq. (46) are real and equal. They are at $s_{1,2} = -R_t/m_t$. The corresponding impulse response is equal to

$$h(t) = K_1 t e^{s_1 t}. \quad (54)$$

5.1.3 Real and Separate Poles

If there is sufficient damping ($R_t^2 > 4m_t k_t$), and this is typical for high-*Bl* drivers, then the poles of Eq. (46) become real and separate. They are at

$$s_{1,2} = -\frac{R_t}{m_t} \pm \sqrt{\left(\frac{R_t}{m_t}\right)^2 - \frac{4k_t}{m_t}}. \quad (55)$$

The corresponding impulse response is equal to

$$h(t) = \frac{K_1}{s_2 - s_1}(e^{s1t} - e^{s2t}). \quad (56)$$

Fig. 13 (dashed curve) shows the impulse response curve [using Eq. (56)] for a high-*Bl* driver with $Bl = 22$ N/A. For this particular value of *Bl,* and other parameters used for this curve, the poles are at $s_1/(2\pi) = 1.72$ kHz and $s_2/(2\pi) = 4.3$ Hz. This 4.3-Hz value is so low that is not visible in the plot of Fig. 4. Therefore it appears that the dashed curve in Fig. 4 has slope +1. This is very uncommon for loudspeakers; however, below 4.3 Hz it has slope +2. This phenomenon was also discussed in [23].

6 DISCUSSION

The equivalent volume of a loudspeaker is given by

$$V_{as} = \frac{\rho c^2 (\pi a^2)^2}{k_d}. \quad (57)$$

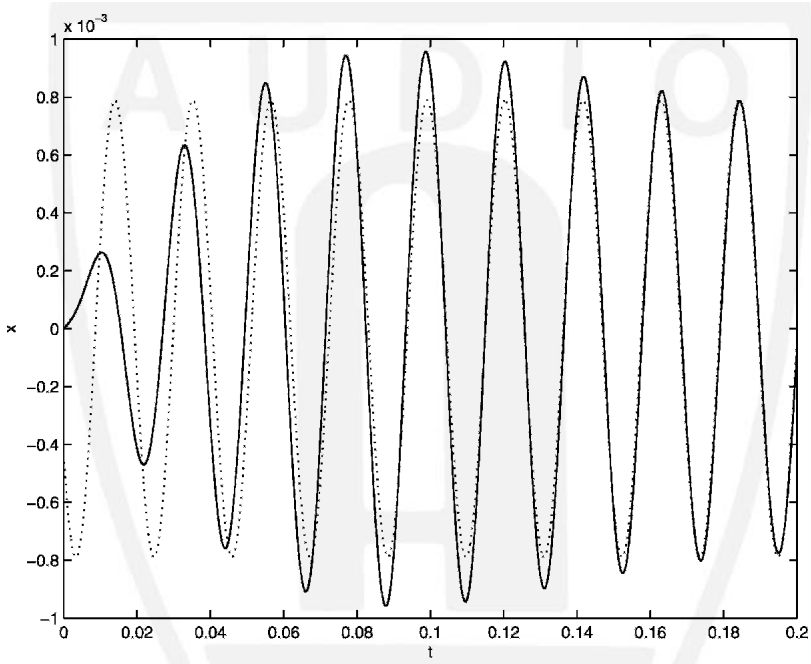

Fig. 12. Displacement of driver MM3c with low *Bl* value of 1.2 N/A (——). All other parameters are kept as given in Table 2; all with 1 W input power. Frequency of driving signal $\omega_s/(2\pi) = 47$ Hz, which is 1.1 times the driver resonance frequency $f_0 = 43$ Hz. Stationary value of displacement (· · · ·).

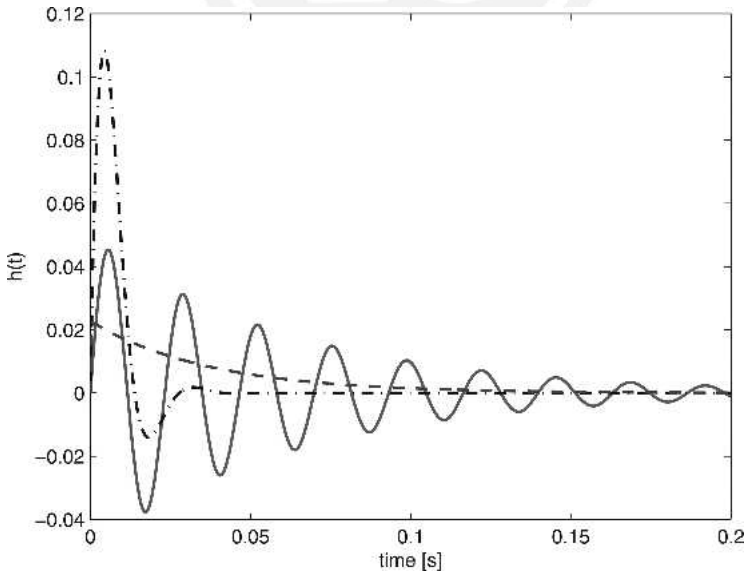

Fig. 13. Impulse response of cone displacement for driver MM3c with three *Bl* values: low $Bl = 1.2$ (——), medium $Bl = 5$ (- · - · -), and high $Bl = 22$ N/A (- - -). All other parameters are kept as given in Table 2; all with 1 W input power.

For a given volume of the enclosure, the corresponding k_B of the "air spring" can be calculated from Eq. (3). Mounting a loudspeaker in a cabinet will increase the total spring constant by an amount given by Eq. (3) and will subsequently increase the resonance frequency of the system. To compensate for this bass loss, the moving mass has to be increased. Thus $\sqrt{k_t m_t}$ is increased, which raises Q_e [see Eq. (13)]. Then *Bl* must be increased in order to preserve the original value of Q_e. The original frequency response is then maintained, but at the cost of a more expensive magnet and a loss in efficiency. This is the designer's dilemma: high efficiency or small enclosure? To meet the demand for a certain cutoff frequency, the enclosure volume must be greater. Alternatively, the efficiency for a given volume will be less than for a system with a higher cutoff frequency.

This dilemma is (partially) solved by using the low-*Bl* concept as discussed in Section 4, however, at the expense of a decreased sound quality and some additional electronics to accomplish the frequency mapping. Many informal listening tests and demonstrations confirmed that the decrease in sound quality appears to be modest—apparently because the auditory system is less sensitive at low frequencies. Also, the other parts of the audio spectrum have a distracting influence on this mapping effect, which has been confirmed during formal listening tests [25], where the detectability of mistuned fundamental frequencies was determined for a variety of realistic complex signals.

7 CONCLUSIONS

The force factor *Bl* plays a very important role in loudspeaker design. It determines the efficiency, the impedance, the SPL response, the temporal response, the weight, and the cost. The choice concerning these parameters depends on the application. High-*Bl* drivers have a high efficiency, but require equalization and a large and heavy magnet system, which makes them less suitable for portable equipment. If the size of the cabinet is of lesser importance, a medium-*Bl* is the simplest solution, because it does not require any other measures. On the other hand, if a very small cabinet and a high efficiency are important, then the low-*Bl* system is to be preferred. A new low-*Bl* driver has been developed which, together with some additional electronics, yields a low-cost, lightweight, flat, and very high-efficiency loudspeaker system for low-frequency sound reproduction.

8 ACKNOWLEDGMENT

John Vanderkooy, during his sabbatical stay at our lab, worked on high-*Bl* loudspeakers, which was an interesting and fruitful time. I'm most indebted to John for his work and enthusiasm on the high-*Bl* project. Also I would like to thank Guido D'Hoogh (Philips Consumer Electronics), Joris Nieuwendijk (Philips Applied Technologies), and Okke Ouweltjes, Jan van Leest, and Jim Oostveen (Philips Research Eindhoven), who gave valuable assistance to the low-*Bl* project. Finally, I wish to thank D. B. (Don) Keele, Jr., Arie Kaizer, and two anonymous reviewers for valuable comments.

9 REFERENCES

[1] R. M. Aarts and C. J. L. van Driel, "Ambient Video, Displays, Audio and Lighting," in *The New Everyday: Views on Ambient Intelligence,* E. Aarts and S. Marzano, Eds. (010 Publ., Rotterdam, The Netherlands, 2003).

[2] R. M. Aarts, "Hardware for Ambient Sound Reproduction," in *Proc. Int. Symp. on Hardware Technology Drivers of Ambient Intelligence* (Veldhoven, The Netherlands, 2004 Dec.), chap. 5.3.

[3] R. M. Aarts, "On the Design and Psychophysical Assessment of Loudspeaker Systems," Ph.D. thesis, Delft University of Technology (Delft, The Netherlands, 1995 Sept.).

[4] H. F. Olson, *Acoustical Engineering* (Van Nostrand, Princeton, NJ, 1957).

[5] L. L. Beranek, *Acoustics* (McGraw-Hill, New York, 1954; reprinted by ASA, 1986).

[6] F. V. Hunt, *Electroacoustics* (Wiley, New York, 1954; reprinted by ASA, 1982).

[7] J. Borwick, Ed., *Loudspeaker and Headphone Handbook* (Butterworths, London, 1988).

[8] J. Merhaut, *Theory of Electroacoustics* (McGraw-Hill, New York, 1981).

[9] A. N. Thiele, "Loudspeakers in Vented Boxes: Part I," *J. Audio Eng. Soc.,* vol. 19, pp. 382–392 (1971 May).

[10] R. H. Small, "Closed-Box Loudspeaker Systems, Part I: Analysis," *J. Audio Eng. Soc.,* vol. 20, pp. 798–808 (1972 Dec.).

[11] D. Clark, "Precision Measurement of Loudspeaker Parameters," *J. Audio Eng. Soc.,* vol. 45, pp. 129–140 (1997 Mar.).

[12] D. B. Keele, Jr., "Maximum Efficiency of Direct-Radiator Loudspeakers," presented at the 91st Convention of the Audio Engineering Society, *J. Audio Eng. Soc.* (*Abstracts*), vol. 39, p. 608 (1991 Dec.), preprint 3193.

[13] D. B. Keele, Jr., "Comparison of Direct-Radiator Loudspeaker System Nominal Power Efficiency vs. True Efficiency with High-*Bl* Drivers," presented at the 115th Convention of the Audio Engineering Society, *J. Audio Eng. Soc.* (*Abstracts*), vol. 51, p. 1224 (2003 Dec.), convention paper 5887.

[14] R. M. Aarts, "High Efficiency Audio Transducer," patent WO2005027570, priority date 09/16/03.

[15] R. M. Aarts, O. Ouweltjes, and D. W. E. Schobben, "Audio Frequency Range Adaptation," patent WO2005027568, priority date 09/16/03.

[16] R. M. Aarts, "High Efficiency Audio Reproduction," patent WO2005027569, priority date 09/16/03.

[17] C. Zuccatti, "Direct-Radiator Loudspeaker Efficiency at Fundamental Resonance," *J. Audio Eng. Soc.,* vol. 53, pp. 307–313 (2005 Apr.).

[18] C. Zuccatti, "Low-DC-Resistance, Low-Frequency Loudspeaker Enclosures," *J. Audio Eng. Soc.* (*Engineering Reports*), vol. 53, pp. 419–428 (2005 May).

[19] P. M. Morse and K. U. Ingard, *Theoretical Acoustics* (McGraw-Hill, New York, 1968).

[20] L. E. Kinsler, A. R. Frey, A. B. Coppens, and J. V. Sanders, *Fundamentals of Acoustics* (Wiley, New York, 1982).

[21] M. Abramowitz and I. A. Stegun, *Handbook of Mathematical Functions* (Dover, New York, 1972).

[22] R. M. Aarts and A. J. E. M. Janssen, "Approximation of the Struve Function H_1 Occurring in Impedance Calculations," *J. Acoust. Soc. Am.,* vol. 113, pp. 2635–2637 (2003 May).

[23] J. Vanderkooy, P. M. Boers, and R. M. Aarts, "Direct-Radiator Loudspeaker Systems with High *Bl,*" *J. Audio Eng. Soc.,* vol. 51, pp. 625–634 (2003 July/Aug.).

[24] E. Larsen and R. M. Aarts, *Audio Bandwidth Extension. Application of Psychoacoustics, Signal Processing and Loudspeaker Design* (Wiley, New York, 2004).

[25] N. Le Goff, R. M. Aarts, and A. G. Kohlrausch, "Thresholds for Hearing Mistuning of the Fundamental Component in a Complex Sound," in *Proc. 18th Int. Cong. on Acoustics* (*ICA2004*) (Kyoto, Japan, 2004), paper Mo.P3.21, p. I-865.

THE AUTHOR

Ronald Aarts was born in Amsterdam, the Netherlands, in 1956. He received a B.Sc. degree in electrical engineering in 1977, and a Ph.D. degree in physics from the Delft University of Technology, Delft, the Netherlands, in 1995.

Dr. Aarts joined the Optics group at Philips Research Laboratories, Eindhoven, the Netherlands, in 1977, there he initially investigated servos and signal processing for use in both Video Long Play players and Compact Disc players. In 1984 he joined the Acoustics group and worked on the development of CAD tools and signal processing for loudspeaker systems. In 1994 he became a member of the Digital Signal Processing (DSP) group and has led research projects on the improvement of sound reproduction by exploiting DSP and psychoacoustical phenomena. In 2003 he became a research fellow and extended his interests in engineering to medicine and biology.

Dr. Aarts has published a large number of papers and reports and holds over seventy granted and pending U.S. patents in these fields. He has served on a number of organizing committees and as chair for various international conventions. He is a senior member of the IEEE, a fellow and governor of the AES, and a member of the NAG (Dutch Acoustical Society), the Acoustical Society of America, and the VvBBMT (Dutch Society for Biophysics and Biomedical Engineering).